JACS
JOURNAL OF THE AMERICAN CHEMICAL SOCIETY
Communication
pubs.acs.org/JACS

A New Crystal Structure of Au_{36} with a Au_{14} Kernel Cocapped by Thiolate and Chloride

Sha Yang,[†] Jinsong Chai,[†] Yongbo Song, Xi Kang, Hongting Sheng, Hanbao Chong, and Manzhou Zhu*

Department of Chemistry and Centre for Atomic Engineering of Advanced Materials, Anhui University, Hefei, Anhui 230601, China

Supporting Information

ABSTRACT: This study presents a new crystal structure of a gold nanocluster coprotected by thiolate and chloride, with the formula of $Au_{36}(SCH_2Ph\text{-}^tBu)_8Cl_{20}$. This nanocluster is composed of a Au_{14} core with two Cl atoms, a pair of pentameric $Au_5(SCl_5)$ staple motifs, and a pair of hexameric $Au_6(S_3Cl_4)$ motifs. It is noteworthy that the "Au−Cl−Au" staple motifs are observed for the first time in thiolate protected gold nanoclusters. More importantly, the formation of the $Cl-Au_3$ motifs is found to be mainly responsible for the configuration of the gold nanocluster. This work will offer a new perspective to understand how the ligands affect the crystal structure of gold nanocluster.

Metal nanoclusters protected by ligands have attracted intensive research interest as a new class of material in nanoscience.[1] In this context, gold nanoclusters protected by phosphines[2−11] or thiolates[12−25] have made breakthroughs in both synthesis and structure determination. The structures of phosphine-protected nanoclusters such as Au_5, Au_7, Au_8, Au_{11}, Au_{13}, and Au_{39} were previously reported, but their stability is not satisfactory.

In recent years, Au nanoclusters protected by thiolate have been extensively studied due to their higher stability than phosphine protected ones. To date, a number of crystal structures of the gold−thiolate nanoclusters such as Au_{18}, Au_{20}, Au_{23}, Au_{24}, Au_{25}, Au_{28}, Au_{30}, Au_{36}, Au_{38}, Au_{102}, and Au_{133} have been characterized.[12−25] Recently, the alkyne and phosphine protected gold nanoclusters such as $[Au_{23}(Ph_3P)_6(PhC{\equiv}C)_9](SbF_6)_2$ and selenolate protected gold nanoclusters such as $Au_{24}(SeR)_{20}$ have also been reported. Their distinct structures from the related thiolate protected ones (i.e., $Au_{23}(SR)_{16}$ and $Au_{24}(SR)_{20}$) imply that the ligands may affect the crystal structure.[26,27] Despite these developments, the organic ligands located on the surface of nanoclusters always result in high steric hindrance and thus are unfavorable for practical applications such as catalysis. Therefore, the development of gold nanoclusters stabilized by small ligands (e.g., Cl−, Br−, SH_2, or SCN−) is desirable. These ligands can sufficiently stabilize the nanocluster and enable the exposure of the surface gold atoms as well.[28,29] A recent density functional theory study by Jiang et al. shows the high similarity between $Au_{25}Cl_{18}^-$ and $Au_{25}(SR)_{18}^-$ in various aspects, such as Au−X distances, X−Au−X angles, band gap, and frontier orbitals (X = Cl or SR).[28] Accordingly, the gold nanoclusters with chloride could possibly be discovered.

Herein, we report the synthesis and crystal structure of a new $Au_{36}(SCH_2Ph\text{-}^tBu)_8Cl_{20}$ nanocluster (**Au_{36}-Cl** for short). The structure of the **Au_{36}-Cl** comprises a Au_{14} inner core with two Cl atoms, a pair of pentameric $Au_5(SCl_5)$ staple motifs, and a pair of hexamer $Au_6(S_3Cl_4)$ motifs. Compared with the $Au_{36}(SR)_{24}$ nanocluster previously reported by the Jin group, the **Au_{36}-Cl** nanocluster shows four distinct differences: (a) eight free electrons; (b) dissimilar optical properties; (c) a Au_{14} core consisting of two Au_7 units; and (d) unique "Au_nCl_m" staple motifs, which is observed for the first time in thiolate protected gold nanoclusters. (The Cl atoms have been analyzed by X-ray photoelectron spectroscopy (Figure S1).)

The synthetic details are provided in the Supporting Information (SI). In a typical reaction, $HAuCl_4{\cdot}3H_2O$ was dissolved in water and then phase-transferred to CH_2Cl_2 with the aid of tetraoctylammonium bromide (TOAB). Then, $HSCH_2Ph\text{-}^tBu$ was added, and 2 seconds later a borane *tert*-butylamine complex was added. After 1 h, the aqueous phase was removed, and the organic phase was rotavaporated at room temperature. The product was washed several times with CH_3OH. The optical absorption spectrum of **Au_{36}-Cl** nanoclusters (dissolved in CH_2Cl_2) shows three stepwise peaks at 365, 420, and 502 nm (Figure 1). Of note, the optical spectrum

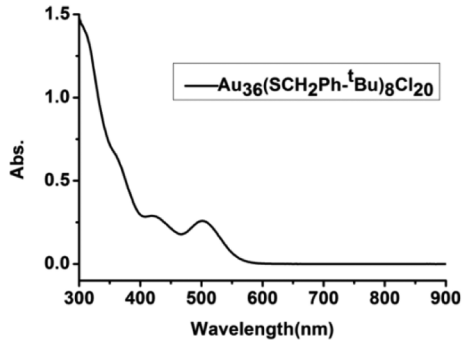

Figure 1. Optical absorption spectrum of **Au_{36}-Cl nanocluster**.

of the **Au_{36}-Cl** is distinct from that of $Au_{36}(SR)_{24}$ (with peaks at 375 and 570 nm). We also have performed stability tests of **Au_{36}-Cl** nanocluster, e.g. under thermal or oxidizing/reducing environments. The results indicate that the **Au_{36}-Cl** is stable under relatively weak reducing/oxidizing and thermal conditions while becoming unstable under strong reducing/

Received: June 16, 2015
Published: August 7, 2015

DOI: 10.1021/jacs.5b06235
J. Am. Chem. Soc. 2015, 137, 10033−10035

oxidizing or thermal environments. The details are provided in the Supporting Information (SI).

The salmon pink crystals of **Au_{36}-Cl** were obtained via crystallization in CH_2Cl_2/ethanol over 2−3 days. The structure of **Au_{36}-Cl** was determined by X-ray crystallography (Figure 2). We found that the structure of the **Au_{36}-Cl** has a triclinic space group $P\bar{1}$ (Table S1).

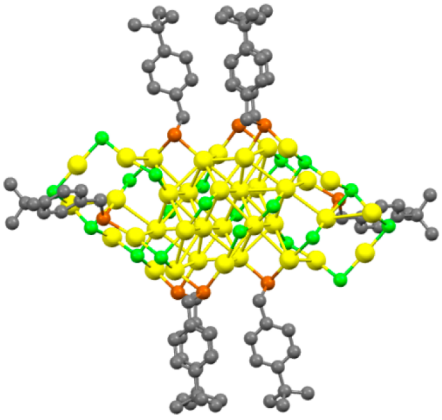

Figure 2. Crystal structure of the **Au_{36}-Cl** nanocluster (Color labels: yellow = Au, brown = S, light green = Cl, gray = C; all H atoms are not shown).

To find out the details of the atom-packing mode in **Au_{36}-Cl**, we focus on the $Au_{36}S_8Cl_{20}$ framework. As shown in Figure 3,

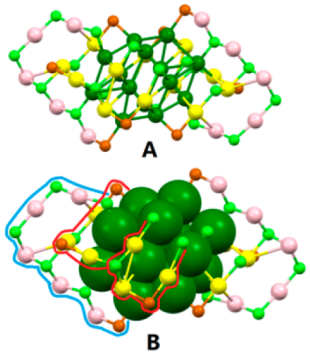

Figure 3. (A) Framework of the **Au_{36}-Cl** nanocluster with the Au_{14} kernel highlighted in green. (B) New staple motifs in the **Au_{36}-Cl**: $Au_5(SCl_5)$ staple and $Au_6(S_3Cl_4)$ staple (Color labels: green/yellow, pink = kernel/surface Au atoms; brown = S; light green = Cl).

the $Au_{36}S_8Cl_{20}$ can be viewed as a Au_{14} core (Figure 3A, highlighted with green) covered with two Cl atoms, a pair of pentameric $Au_5(SCl_5)$ staple motifs (Figure 3B; the left one is labeled with light blue curve), and a pair of hexameric $Au_6(S_3Cl_4)$ staple motifs (Figure 3B, labeled with the red curve). The $Au_{36}(SR)_{24}$ has a Au_{28} kernel (FCC-type core) which is protected by 12 S atoms and four dimeric staple motifs (−SR−Au−SR−Au−SR−). To our knowledge, these "Au−Cl−Au" staple motifs are observed in thiolate protected gold nanoclusters for the first time. Furthermore, the whole structure of the **Au_{36}-Cl** is centrosymmetric.

For a more detailed anatomy of the total structure, we start with the Au_{14} kernel (Figure 4C, side view). From the side view, the Au_{14} kernel can be divided into two layers (Figure 4A and 4B). Each of the two layers contains 7 Au atoms, and forms

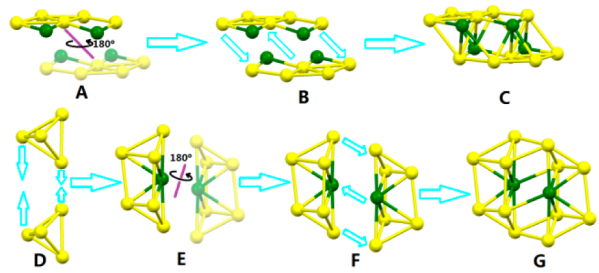

Figure 4. Au_{14} kernel structure of the **Au_{36}-Cl** nanocluster (Color labels: yellow/green = Au).

a hexagon with one Au atom at the center of the hexagon. As shown in Figure 4A, the two layers are centrosymmetric. The Au atoms are almost in the same plane (the angle sum of hexagon: 719.56°) (Figure 4B). The Au−Au distances in the hexagon range from 2.70 to 3.31 Å. Alternatively, the Au_{14} kernel can also be divided into two jointed Au_7 units without sharing Au atoms (Figure 4G, top view). Herein, each of the Au_7 units can be viewed as two tetrahedral Au_4 units sharing one vertex (7 = 4 + 4 − 1, Figure 4D). And then, the Au_7 units join together without sharing Au atoms (Figure 4E). Furthermore, there are two more Cl atoms at the surface of the tetrahedral Au_4 units (Figure S2), which induce longer Au−Au bond lengths (average: 2.99 Å) than those of the other tetrahedral Au_4 units (average: 2.76 Å) without the Cl atoms.

The Au_{14} kernel is protected by a pair of pentameric $Au_5(SCl_5)$ and a pair of hexameric $Au_6(S_3Cl_4)$ staple motifs (Figure 3B). These staple motifs containing Cl atoms are observed for the first time in thiolate protected gold nanoclusters. Some structural differences between $Au_n(SR)_m$ and $Au_n(Cl/SR)_m$ motifs are worthy of comment (vide supra).

As shown in Figure 5A, the pentameric $Au_5(SCl_5)$ motif with a linear "SR−Au−Cl−Au−Cl−Au−Cl−Au−Cl−Au−Cl" struc-

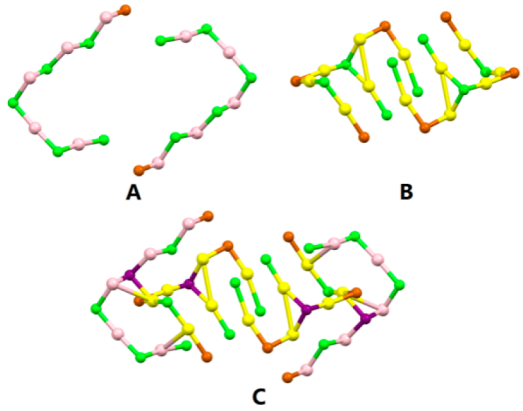

Figure 5. Two kinds of staple motifs in **Au_{36}-Cl** nanocluster (Color labels: yellow/pink = Au, brown = S; light green/purple = Cl).

ture can be easily identified from **Au_{36}-Cl**. In this staple motif, Cl is either triply or doubly coordinated with the Au atoms. The bond lengths of Au−Cl in the pentameric $Au_5(SCl_5)$ staple motifs range from 2.133 to 2.334 Å (average: 2.264 Å) and are slightly shorter than those of the typical Au−S bonds on average (2.31 Å). Furthermore, due to the formation of the Cl−Au_3 (Figure 5C), the bond angles of Cl−Au−Cl can be generally categorized into two groups: (i) from 159.57° to 175.87° (almost linear), which are similar to that of S−Au−S; (ii) from 95° to 109.20°, which make the staple motifs more

DOI: 10.1021/jacs.5b06235
J. Am. Chem. Soc. 2015, 137, 10033−10035

flexible than the corresponding $Au_n(SR)_m$ or $Au_n(SeR)_m$ staple motifs. The same phenomena (i.e., two types of Cl−Au−Cl bond angles and formation of the Cl−Au_3 motifs) were also observed in the hexameric $Au_6(S_3Cl_4)$ staple motifs (Figure 5B). It is notable that there is a branch in the $Au_6(S_3Cl_4)$ hexamer, which is unprecedented in the $Au_n(SR)_m$ or $Au_n(SeR)_m$. In view of the entire structure, both the coordination of the staple motifs to the Au_{14} kernel and the Au−Au/Au-Cl bonds between the two types of staple motifs (Figure 5C, highlighted with purple) contribute to the stability of the **Au_{36}-Cl** nanocluster. Meanwhile, the formation of Cl−Au_3 plays an important role in the whole structure of this nanocluster.

In summary, this study reports the crystal structure of a $Au_{36}(SCH_2Ph\text{-}^tBu)_8Cl_{20}$ nanocluster coprotected by thiolate and chlorine. This nanocluster consists of a Au_{14} core with two Cl atoms, a pair of pentameric $Au_5(SCl_5)$ staple motifs, and a pair of hexamer $Au_6(S_3Cl_4)$ staple motifs. The "Au−Cl−Au" staple motifs are for the first time reported in thiolate protected gold nanoclusters. Of note, the formation of the Cl−Au_3 is primarily responsible for the configuration of the gold nanocluster. The distinct optical properties and crystal structures of **Au_{36}-Cl** and the previously reported $Au_{36}(SR)_{24}$ unambiguously imply the important role of the ligand effect.

■ ASSOCIATED CONTENT

Supporting Information

The Supporting Information is available free of charge on the ACS Publications website at DOI: 10.1021/jacs.5b06235.

Detailed information about the synthesis, Figures S1 and S2, stability experiments (PDF)

X-ray analysis of $Au_{36}(SCH_2Ph\text{-}^tBu)_8Cl_{20}$ (CIF)

■ AUTHOR INFORMATION

Corresponding Author

*zmz@ahu.edu.cn

Author Contributions

†S.Y. and J.C. contributed equally.

Notes

The authors declare no competing financial interest.

■ ACKNOWLEDGMENTS

We acknowledge financial support by the NSFC (21072001, 21372006), the Ministry of Education and Ministry of Human Resources and Social Security, the Education Department of Anhui Province, Anhui Province International Scientific and Technological Cooperation Project, and 211 Project of Anhui University.

■ REFERENCES

(1) (a) Schmid, G. *J. Cluster Sci.* **2014**, *25*, 29. (b) Knoppe, S.; Bürgi, T. *Acc. Chem. Res.* **2014**, *47*, 1318. (c) Luo, Z.; Castleman, A. *Acc. Chem. Res.* **2014**, *47*, 2931.

(2) McPartlin, M.; Mason, R.; Malatesta, L. *J. Chem. Soc. D* **1969**, *7*, 334.

(3) Manassero, M.; Naldini, L.; Sansoni, M. *J. Chem. Soc., Chem. Commun.* **1979**, *9*, 385.

(4) Briant, C. E.; Theobald, B. R. C.; White, J. W.; Bell, L. K.; Mingos, D. M. P.; Welch, A. J. *J. Chem. Soc., Chem. Commun.* **1981**, *5*, 201.

(5) (a) Shichibu, Y.; Kamei, Y.; Konishi, K. *Chem. Commun.* **2012**, *48*, 7559. (b) Shichibu, Y.; Suzuki, K.; Konishi, K. *Nanoscale* **2012**, *4*, 4125. (c) Shichibu, Y.; Konishi, K. *Small* **2010**, *6*, 1216. (d) Shichibu, Y.; Konishi, K. *Inorg. Chem.* **2013**, *52*, 6570. (e) Shichibu, Y.; Zhang, M.; Kamei, Y.; Konishi, K. *J. Am. Chem. Soc.* **2014**, *136*, 12892.

(6) Wan, X. K.; Lin, Z. W.; Wang, Q. *J. Am. Chem. Soc.* **2012**, *134*, 14750.

(7) Gutrath, B. S.; Oppel, I. M.; Presly, O.; Beljakov, I.; Meded, V.; Wenzel, W.; Simon, U. *Angew. Chem., Int. Ed.* **2013**, *52*, 3529.

(8) Teo, B. K.; Shi, X.; Zhang, H. *J. Am. Chem. Soc.* **1992**, *114*, 2743.

(9) Yanagimoto, Y.; Negishi, Y.; Fujihara, H.; Tsukuda, T. *J. Phys. Chem. B* **2006**, *110*, 11611.

(10) Chen, J.; Zhang, Q.; Bonaccorso, T. A.; Williard, P. G.; Wang, L. *J. Am. Chem. Soc.* **2014**, *136*, 92.

(11) Mckenzie, L. C.; Zaikova, T. O.; Hutchison, J. E. *J. Am. Chem. Soc.* **2014**, *136*, 13426.

(12) Jadzinsky, P. D.; Calero, G.; Ackerson, C. J.; Bushnell, D. A.; Kornberg, R. D. *Science* **2007**, *318*, 430.

(13) Heaven, M. W.; Dass, A.; White, P. S.; Holt, K. M.; Murray, R. W. *J. Am. Chem. Soc.* **2008**, *130*, 3754.

(14) Zhu, M.; Aikens, C. M.; Hollander, F. J.; Schatz, G. C.; Jin, R. *J. Am. Chem. Soc.* **2008**, *130*, 5883.

(15) Qian, H.; Eckenhoff, W. T.; Zhu, Y.; Pintauer, T.; Jin, R. *J. Am. Chem. Soc.* **2010**, *132*, 8280.

(16) Crasto, D.; Malola, S.; Brosofsky, G.; Dass, A.; Hakkinen, H. *J. Am. Chem. Soc.* **2014**, *136*, 5000.

(17) Zeng, C.; Qian, H.; Li, T.; Li, G.; Rosi, N. L.; Yoon, B.; Barnett, R. N.; Whetten, R. L.; Landman, U.; Jin, R. *Angew. Chem., Int. Ed.* **2012**, *51*, 13114.

(18) Zeng, C.; Li, T.; Das, A.; Rosi, N. L.; Jin, R. *J. Am. Chem. Soc.* **2013**, *135*, 10011.

(19) Das, A.; Li, T.; Li, G.; Nobusada, K.; Zeng, C.; Rosi, N. L.; Jin, R. *Nanoscale* **2014**, *6*, 6458.

(20) Das, A.; Li, T.; Nobusada, K.; Zeng, C.; Rosi, N. L.; Jin, R. *J. Am. Chem. Soc.* **2013**, *135*, 18264.

(21) Zeng, C.; Liu, C.; Chen, Y.; Rosi, N. L.; Jin, R. *J. Am. Chem. Soc.* **2014**, *136*, 11922.

(22) Chen, S.; Wang, S.; Zhong, J.; Song, Y.; Zhang, J.; Sheng, H.; Pei, Y.; Zhu, M. *Angew. Chem., Int. Ed.* **2015**, *54*, 3145.

(23) Das, A.; Liu, C.; Byun, H. Y.; Nobusada, K.; Zhao, S.; Rosi, N.; Jin, R. *Angew. Chem., Int. Ed.* **2015**, *54*, 3140.

(24) Zeng, C.; Chen, Y.; Kirschbaum, K.; Appavoo, K.; Sfeir, M. Y.; Jin, R. *Sci. Adv.* **2015**, *1*, e1500045.

(25) Dass, A.; Theivendran, S.; Nimmala, P. R.; Kumara, C.; Jupally, V. R.; Fortunelli, A.; Sementa, L.; Barcaro, G.; Zuo, X.; Noll, B. C. *J. Am. Chem. Soc.* **2015**, *137*, 4610.

(26) (a) Wan, X.; Tang, Q.; Yuan, S.; Jiang, D.; Wang, Q. *J. Am. Chem. Soc.* **2015**, *137*, 652. (b) Wan, X.; Yuan, S.; Tang, Q.; Jiang, D.; Wang, Q. *Angew. Chem.* **2015**, *127*, 6075.

(27) (a) Song, Y.; Wang, S.; Zhang, J.; Kang, X.; Chen, S.; Li, P.; Sheng, H.; Zhu, M. *J. Am. Chem. Soc.* **2014**, *136*, 2963. (b) Song, Y.; Fu, F.; Zhang, J.; Chai, J.; Kang, X.; Li, P.; Li, S.; Zhou, H.; Zhu, M. *Angew. Chem., Int. Ed.* **2015**, *54*, 8430.

(28) Jiang, D.; Walter, M. *Nanoscale* **2012**, *4*, 4234.

(29) Lugo, G.; Schwanen, V.; Fresch, B.; Remacle, F. *J. Phys. Chem. C* **2015**, *119*, 10969.

DOI: 10.1021/jacs.5b06235
J. Am. Chem. Soc. 2015, 137, 10033−10035